Venkatesh Suriyanarayanan[1]
Department of Mechanical Engineering,
Imperial College London,
London SW7 2AZ, UK
e-mail: v.suriyanarayanan16@imperial.ac.uk

Quentin Rendu
Department of Mechanical Engineering,
Imperial College London,
London SW7 2AZ, UK
e-mail: q.rendu@imperial.ac.uk

Mehdi Vahdati
Department of Mechanical Engineering,
Imperial College London,
London SW7 2AZ, UK
e-mail: m.vahdati@imperial.ac.uk

Loic Salles
Department of Mechanical Engineering,
Imperial College London,
London SW7 2AZ, UK
e-mail: l.salles@imperial.ac.uk

Effect of Manufacturing Tolerance in Flow Past a Compressor Blade

This paper presents the effect of manufacturing tolerance on performance and stability boundaries of a transonic fan using a Reynolds-averaged Navier–Stokes simulation. The effects of tip gap and stagger angle variations were analyzed through a series of single passage and double passage simulation; based on which an optimal arrangement was proposed for random tip gap and random stagger angle variation for a whole annulus rotor. All simulations were carried out using NASA rotor 67 as a test case and AU3D as an in-house computational fluid dynamics solver. Results illustrate that the stagger angle variation mainly affects efficiency and its circumferential variation must be as smooth as possible. Furthermore, the tip gap variation affects the stability boundary as well as performance and its optimal configuration mandates a zigzag arrangement of blades around the annulus, i.e., larger tip gap between two smaller ones. [DOI: 10.1115/1.4052600]

Keywords: compressor stall, surge, and operability, computational fluid dynamics (CFD), fan, compressor

1 Introduction

A real-world system is seldom deterministic in nature. There is always an element of uncertainty present in the parameters that define the system. The uncertainties in a turbomachinery environment can arise during manufacturing of different components, during assembly of these components, due to varying atmospheric conditions and operating conditions. Figures 1(*a*)–1(*c*) represent the types of uncertainty introduced due to manufacturing tolerance in compressor blades while Fig. 1(*d*) showing an eccentric rotor is a classic case of uncertainty introduced due to a whirling shaft. Figure 1(*e*) shows casing ovalization [1] which is introduced due to extreme operating conditions resulting in a distorted geometry. It is noteworthy that both these uncertainties, namely, Figs. 1(*d*) and 1(*e*), introduce non-axisymmetric tips gaps around the annulus of the compressor.

There is an inherent variation between the manufactured compressor blades due to limited precision of machining. Manufacturing tolerance prescribes the limits of allowed variation (upper deviation limit and lower deviation limit) of a manufactured blade from that of the designed blade. The quantification of innumerable uncertainties present in a system is overcome by employing reduced order models wherein only the parameters of interest are considered for further evaluation. The present paper deals with only the uncertainties due to manufacturing tolerance which give rise to differing passage geometry and subsequent performance degradation, as pointed out by Lange et al. [2] using Monte Carlo simulation. Research carried out in the last three decades as listed by Montomoli et al. [3] raises a few open ended questions that few researchers have attempted to tackle, e.g., "Is there an optimal configuration for a given set of random blades? If yes, what is that arrangement?" The authors have addressed the above issues by concentrating on the tip gap (the gap between the casing and the blade) and the stagger angle (the angle between the chord-line and the axis of compressor) as the two parameters affected by manufacturing tolerance.

2 Methods

The simulations were performed using the in-house computational fluid dynamics (CFD) solver AU3D, developed at Imperial College London-VUTC with support from Rolls-Royce. AU3D is a three-dimensional, time-accurate, viscous, compressible Reynolds-averaged Navier–Stokes (RANS) solver that uses Spalart–Allmaras model to evaluate the turbulent eddy viscosity. The solver, implicit and second-order accurate in space and time, has been successfully used to predict the design and off-design conditions [4–6].

Computationally, only a sector of full annulus rotor needs to be considered if all the blades are of same geometry [7]. The sector is called single passage if the domain consists of a single blade; double passage in case of two blades and so on. A full annulus simulation has been performed when random stagger angle and tip gap variation are considered, given the lack of symmetry. The computational domain in this paper consists of (a) inlet duct, (b) rotor, and (c) nozzle. Depending on the case in hand, the rotor could either be single passage, double passage, or full annulus. A variable area nozzle placed downstream of the rotor is adjusted gradually to move the fan operating point from near choke condition to near stall point [8]. The solver operates on a semi-structured mesh with hexahedral elements found around the airfoil and prismatic elements in the rest of the passage. The boundary layer region in rotor-to-rotor grid has a body-fitted O grid while rest of the region is unstructured as seen in Fig. 2(*a*). For more details, please refer to Ref. [9].

Figure 2(*b*) shows a schematic of the radial mesh spacing adopted for griding blades with different tip gaps. With this spacing, the grid on the periodic boundary will be independent of the tip gap size, which simplifies assembling them together. As can be seen, the entire region has been divided into three distinct parts. In part (I), the radial layers for the smallest blade A are chosen such that it is fine towards the blade tip and the hub while gradually coarsens towards the mid span region (this mesh will be used as it is in the largest blade including the intermediate ones). The part (II) starts from the tip gap region for the largest blade up to the blade tip of the smallest blade. This region is equispaced such that all the intermediate tip gap sizes can be covered. All the remaining area up to the casing forms part (III) of the region. The mesh spacing in part (III) has been kept the same as that in part (II) though it can be made finer according to the need.

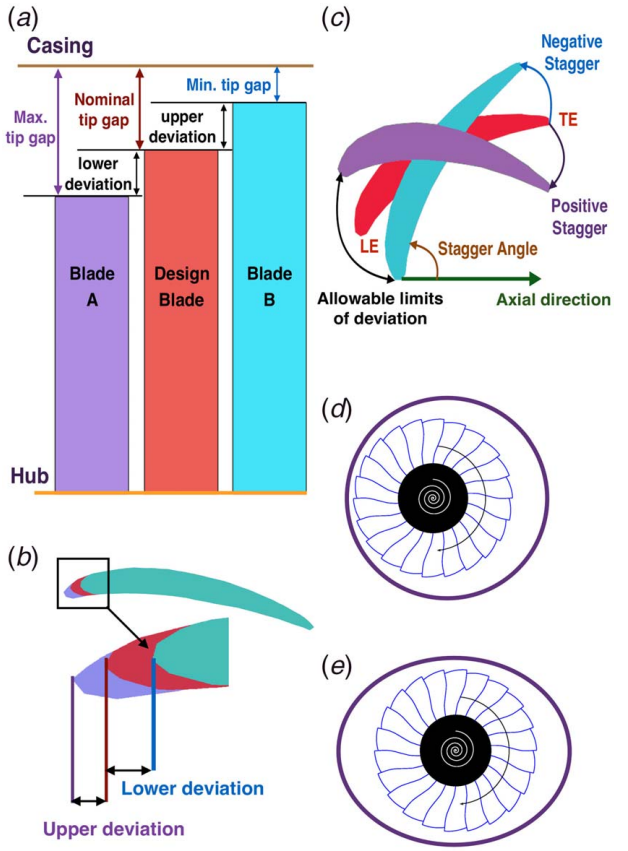

Fig. 1 Schematic of different uncertainties in a turbomachinery environment: (*a*) tip gap tolerance, (*b*) leading edge tolerance, (*c*) stagger angle tolerance, (*d*) eccentric rotor, and (*e*) ovalised casing

3 Test Case and Validation

NASA rotor 67 was used as the test case for all the computations. All the performance curves shown in this paper have been computed using a steady RANS solver. Many papers have adopted the nominal tip gap to be 0.61 mm in their computation [10,11] which can be traced back to Ref. [12]. A summary of all the values of different nominal tip gaps found in the literature is listed in Table 1. Five different tip gap sizes have been used in this paper, namely, 0.3 mm (≈0.188% span), 0.6 mm (≈0.376% span), 0.9 mm (≈0.564% span), 1.2 mm (≈0.752% span), and 1.5 mm (≈0.94% span). The nominal tip gap size is considered to be 0.6 mm (≈0.376% span) which is in line with the previous parametric studies performed using discrete tip gaps in case of NASA rotor 67 [12,15]. Table 2 shows a mesh convergence study been performed to check on the blades with maximum (0.94% span) and minimum (0.188% span) tip gaps in single passage (uniform tip gap) and double passage (alternate arrangement) simulation with mesh refinement in both blade-to-blade direction as well as radial direction (mainly in the tip gap region).

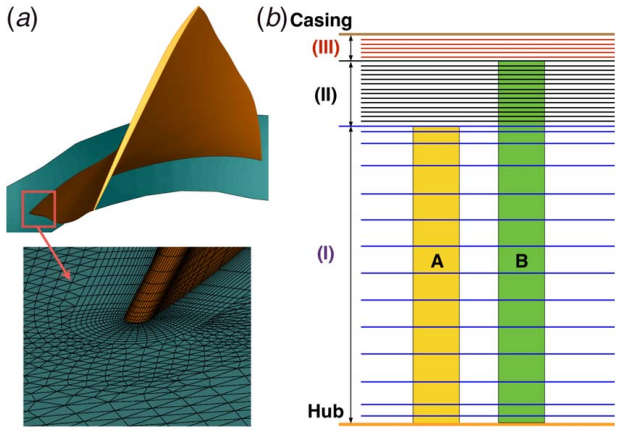

Fig. 2 (*a*) Mesh around the blade and (*b*) radial mesh strategy in case of blades with different tip gaps

Table 1 Uncertainty in nominal tip gap in case of NASA rotor 67

Method	Nominal tip gap	Range of tip gap
Experimental [13]	1 mm	–
Experimental [14]	0.5 mm	–
Computational [15]	0.225 mm	0–1.225 mm
Computational [12]	0.61 mm	0.3–1.22 mm

It can be seen from Fig. 3 that all the three cases have converged at a single passage mesh count of 1 million. Unless otherwise stated, all the performance curves in this paper have been non-dimensionalized with respect to the choke mass flow of the fan with tip gap of 0.188% span (34.7 kg/s). From Fig. 4, it can be seen that the results from the converged solution matched well with the experimentally available results from Ref. [13]. It has to be noted that the latest running tip gap mentioned in Ref. [14] is 0.5 mm (≈0.3% span) and hence the experimental data in Fig. 4 are compared with the results for tip gaps 0.188% span and 0.376% span.

4 Compressor Stagger Angle

There is a dearth of data in open literature pertaining to the aerodynamic study of mis-staggering as most papers concentrate on the aspects of forced response and the mechanism of flutter [16,17]. The available few [7,18,19] on aerodynamic studies mention that the stagger angle variation up to 1 deg is allowed as manufacturing tolerances. When a system is designed for certain tolerance limits and a component exceeds that limit, there is a chance of system failure [20]. Thus any blade that exceeds the prescribed limit is scrapped off, resulting in a financial loss to the manufacturer. With this rationale, the present paper considers the stagger variation to be within ±1.5 deg (±2.2% change of stagger) from the datum stagger, as a way to check if these losses could be mitigated.

The fan blade with nominal tip gap size (0.376% span) was considered and the stagger angle was gradually changed in steps of ±0.73% relative to the datum stagger angle (±0.5 deg). The effects of stagger angle variation on the rotor performance were studied by juxtaposing the five cases: (**I**) single passage domain with nominal blade (also called as 0% change in stagger angle), (**II**) single passage domain with a blade of 2.2% change in stagger angle, (**III**) single passage domain with a blade of −2.2%

Table 2 Mesh used for convergence study

Case (tip gap in % span)	Radial layers (blade + tip gap)	Mesh count (million)
Uniform (0.188%)	85 (82 + 3)	0.5
Uniform (0.188%)	85 (82 + 3)	1
Uniform (0.188%)	130 (118 + 12)	1.5
Uniform (0.94%)	85 (70 + 15)	0.5
Uniform (0.94%)	85 (70 + 15)	1
Uniform (0.94%)	130 (70 + 60)	1.5
Alternate (0.188% and 0.94%)	85 (mixed)	2 × 1
Alternate (0.188% and 0.94%)	130 (mixed)	2 × 1.5

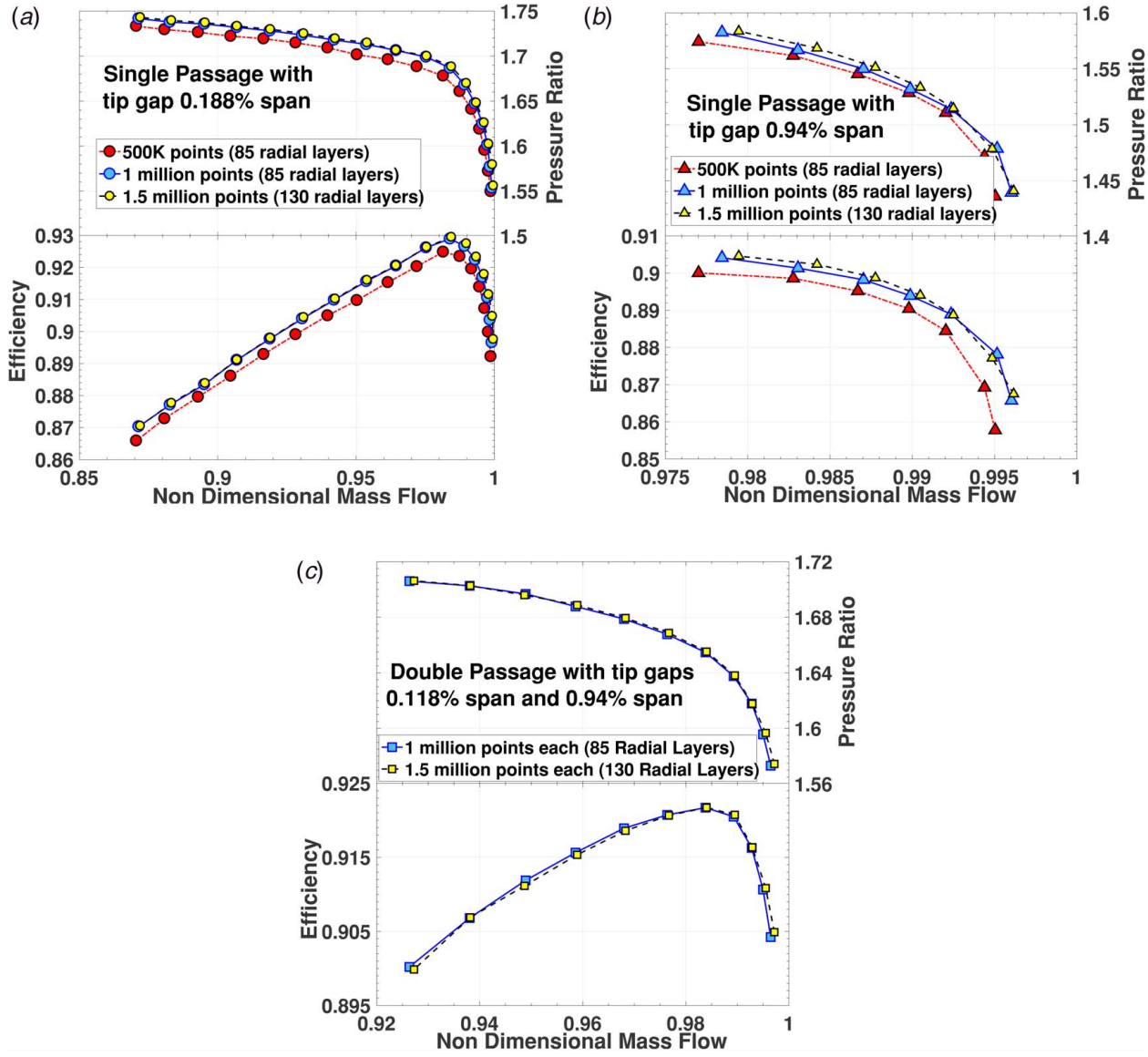

Fig. 3 (*a*) Single passage with tip gap of 0.188% span, (*b*) single passage with tip gap of 0.94% span, and (*c*) double passage with tip gaps of 0.188% and 0.94% span. Mesh convergence plot for different single passage and double passage cases.

change in stagger angle, (**IV**) double passage domain with blades of 0% and 2.2% change in stagger angle, and (**V**) double passage domain with blades of 0% and −2.2% change in stagger angle.

For single passage cases, a blade having ±2.2% change in stagger angle causes the mass flowrate to change by ±2% on either side of the baseline blade as shown in Fig. 5(*a*). Hence, the mass flowrate for each of the above-mentioned case was non-dimensionalized with respective choking mass flowrate which makes a one-to-one comparison between different cases simpler. For brevity, the results of only cases (**I**), (**III**), and (**V**) are presented in Fig. 5(*b*) and a comparison at the non-dimensional mass flowrate of 0.986 (marked by vertical dashed line). These points depict the behavior of the respective cases as they near maximum efficiency. It was seen that the peak efficiency of 92.5% is observed for all the single passage cases; whereas for a double passage case, the peak efficiency drops to about 91.5%. Figure 5(*c*) shows that as the mis-stagger decreases, the peak efficiency increases.

Figures 6(*a*)–6(*c*) show a blade-to-blade view at 75% span for cases (**I**), (**III**), and (**V**), respectively, for static pressure non-dimensionalized with respect to density and velocity. It can be seen that both the single blade cases have symmetric shock

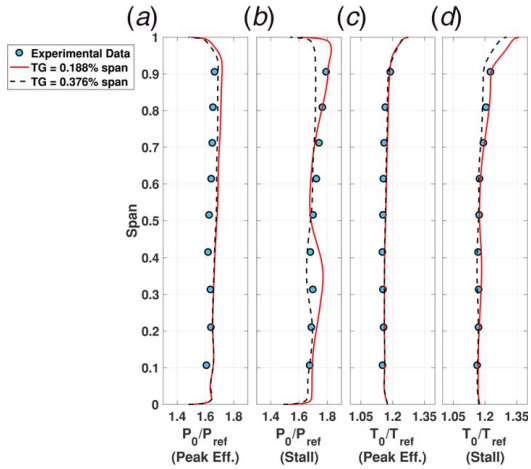

Fig. 4 CFD versus experimental data [13]: (*a*) pressure ratio at peak efficiency, (*b*) pressure ratio at stall, (*c*) temperature ratio at peak efficiency, and (*d*) temperature ratio at stall

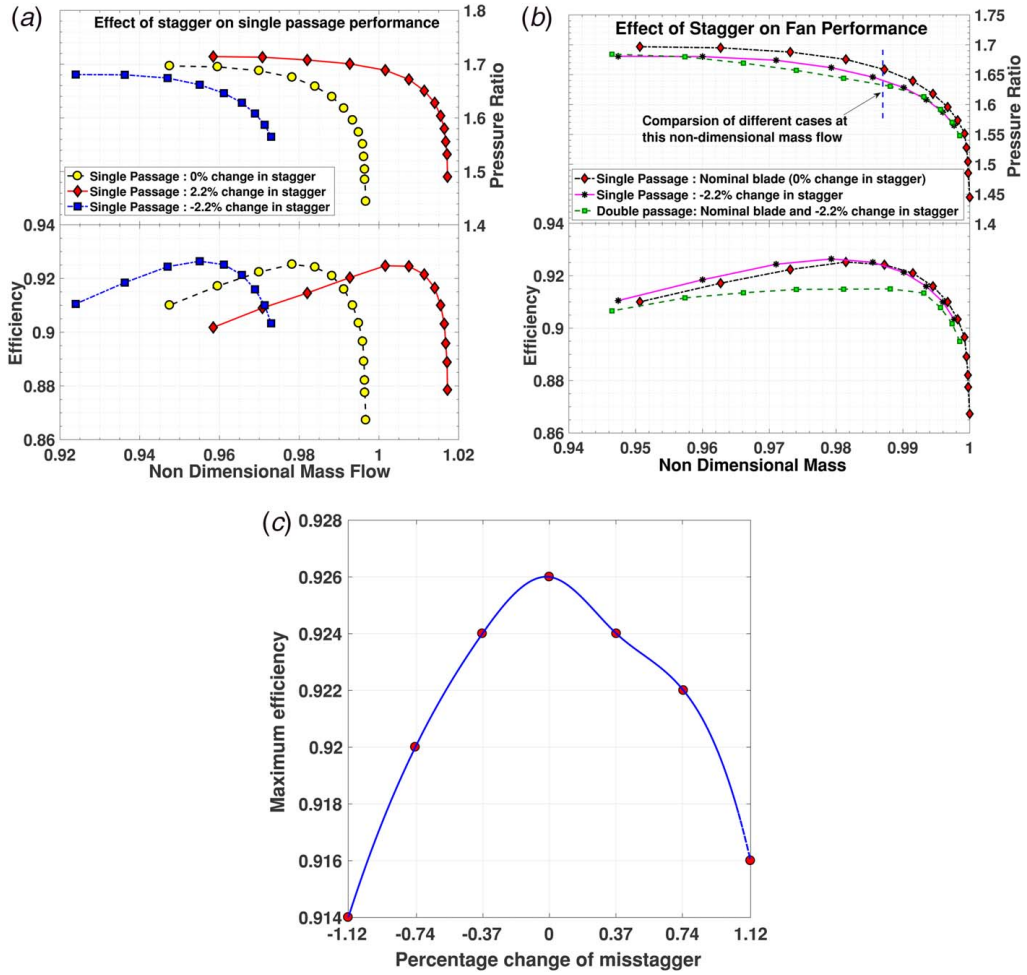

Fig. 5 (*a*) Comparison of fan performance for single passage blade with −2.2% stagger variation, 0% stagger variation, and 2.2% stagger variation, (*b*) effect of stagger variation on single passage uniform staggered blades and double passage non-uniform staggered blades, and (*c*) effect of mis-stagger on maximum efficiency. Changes in fan performance due to stagger variation of blades.

waves which are at the entrance to the blade passage while the case with the blades of different stagger angles has unsymmetrical shock waves [7]. This implies that when one of the blade is having peak efficiency, the other blade is choked and hence the assembly will always be less efficient than the single passage cases. A schematic explanation of the mechanism of change in location of shock wave for a double passage case with different stagger blades is shown in Fig. 7. It can be seen that in case of extreme mis-staggering, one of the passages behaves like a nozzle while the other behaves like a diffuser thus resulting in unsymmetrical shock waves. Moreover, due to asymmetrical aerofoil used in the compressor blades, the area of nozzle and diffuser formed in a double passage computation of case (**IV**) differs from that of case (**V**), thus resulting in different losses in the two cases. This can be clearly seen in Fig. 5(*c*) which shows an unsymmetric shape about the 0% mis-stagger. Thus, the change in passage area because of change in stagger angle results in a drop of performance compared to the baseline case of uniform passage area.

Though the manufacturing tolerances are generally assumed to be Gaussian distribution, in the present paper, a uniform distribution has been assumed. For a closed interval $[a, b]$ the uniform distribution is known to be maximum entropy distribution [21] and as shown in Fig. 8, a uniform distribution represents a design space much better compared to Gaussian distribution which is concentrated towards the mean. Thus, for a given set of uniformly distributed random staggered blades between ±2.2% (as shown in Fig. 9(*a*)) if the arrangement is smooth as shown in Figs. 9(*b*) and 9(*c*), the mis-stagger between successive blades is minimum which maximizes the performance of the compressor. On the other hand, an arrangement that maximizes the variation of stagger angle between two successive blades (as shown in Fig. 9(*d*)) minimizes the performance. This can be clearly seen in

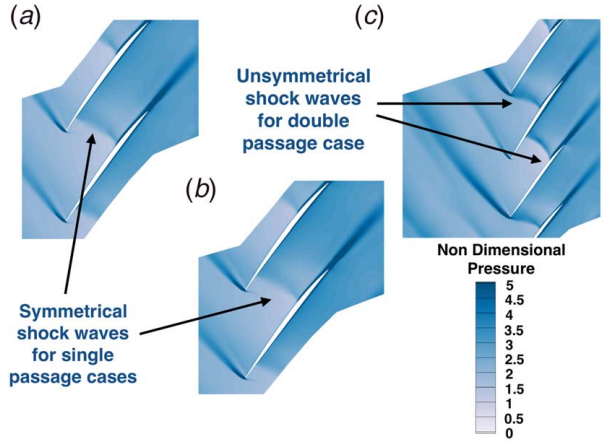

Fig. 6 Shock wave position at 75% span and non-dimensional flowrate of 0.986 for (*a*) single passage 0% stagger change, (*b*) single passage −2.2% stagger change, and (*c*) double passage 0% and −2.2% stagger change

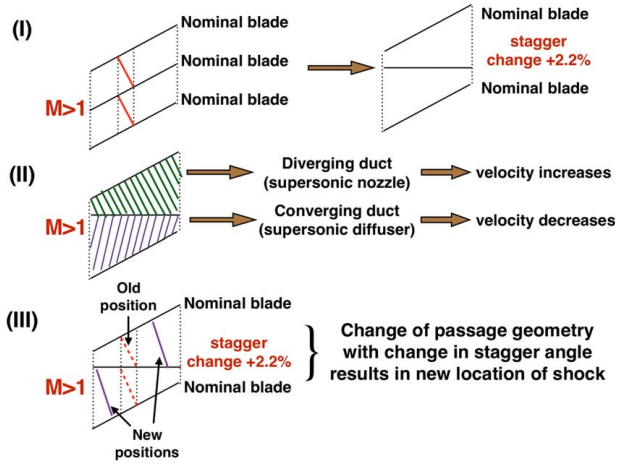

Fig. 7 Schematic showing the change in location of shock with change in stagger angle

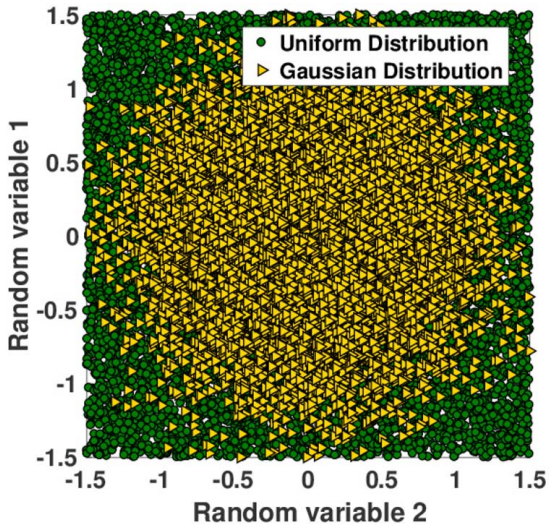

Fig. 8 Scatter plot of two different random distributions within a closed interval

Figs. 10(*a*) and 10(*b*) wherein the sinusoidally and linearly arranged blades around the whole annulus have the best performance; while for the zigzag arrangement it is the worst. The performance of all other random arrangements lie between these two extremities. No difference in the stall mass flow is observed for different configurations. Zheng et al. [19] also observed that the sinusoidal arrangement works best though they have not evaluated the minima of possible performance. While there may be other combinations which give similar high performance, the aim of this paper was to establish a rule of thumb for the best possible arrangement. The sinusoidal arrangement can also have an added advantage of a reduced "Alternate Passage Divergence" as shown in Ref. [22].

5 Compressor Tip Gap

Single passage rotor domain was generated for five different tip clearances: 0.188% span, 0.376% span, 0.564% span, 0.752% span, and 0.94% span. The tip gap variation could also be thought of as a refurbished blade with a smaller stall margin (SM) because of damage at the tip during the course of operation. The **SM** is defined as follows:

$$\mathbf{SM} = \left[\frac{(\mathbf{PR})_{\mathbf{stall}} \times (\dot{\mathbf{m}})_{\mathbf{ref.}}}{(\mathbf{PR})_{\mathbf{ref.}} \times (\dot{\mathbf{m}})_{\mathbf{stall}}} - \mathbf{1}\right] \times \mathbf{100} \tag{1}$$

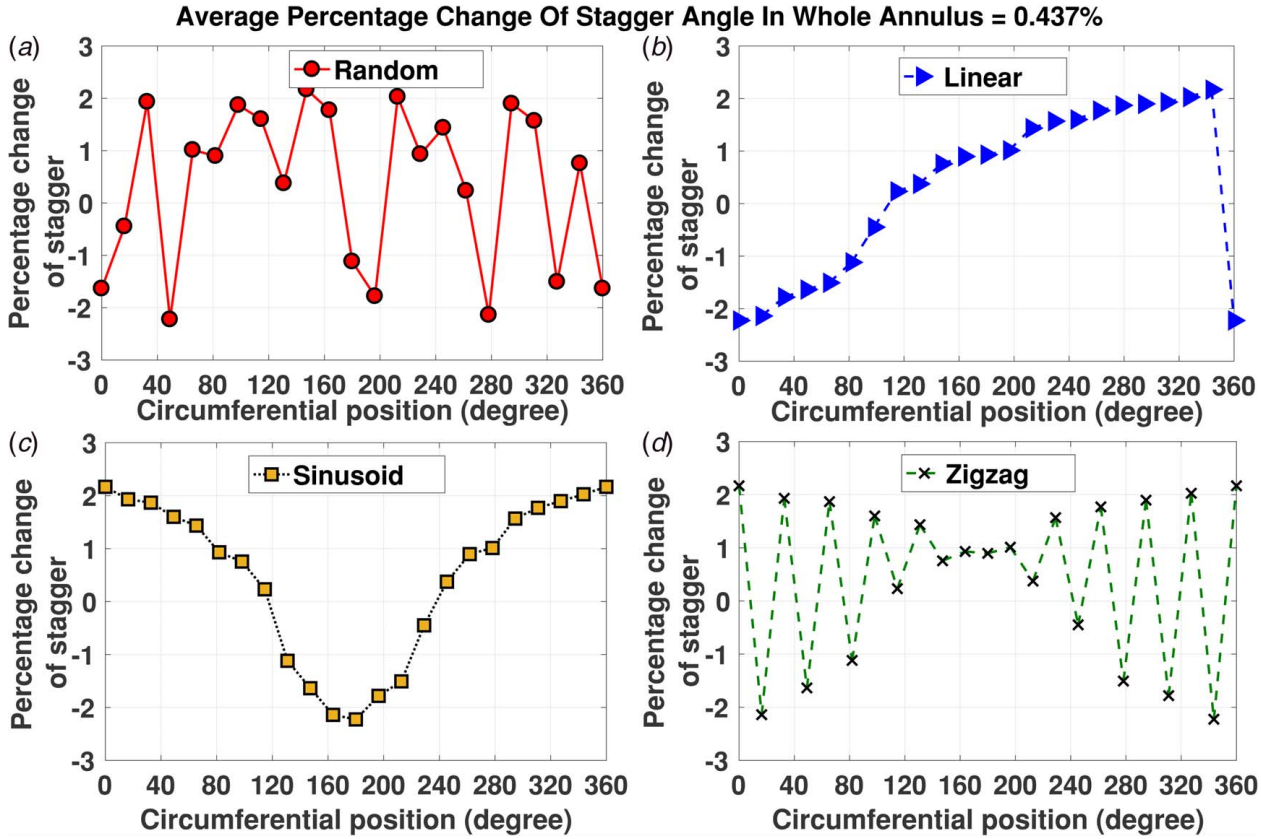

Fig. 9 Different arrangements for same set of random staggered blades with average change of stagger 0.437%: (*a*) random arrangement, (*b*) linear arrangement, (*c*) sinusoid arrangement, and (*d*) zigzag arrangement

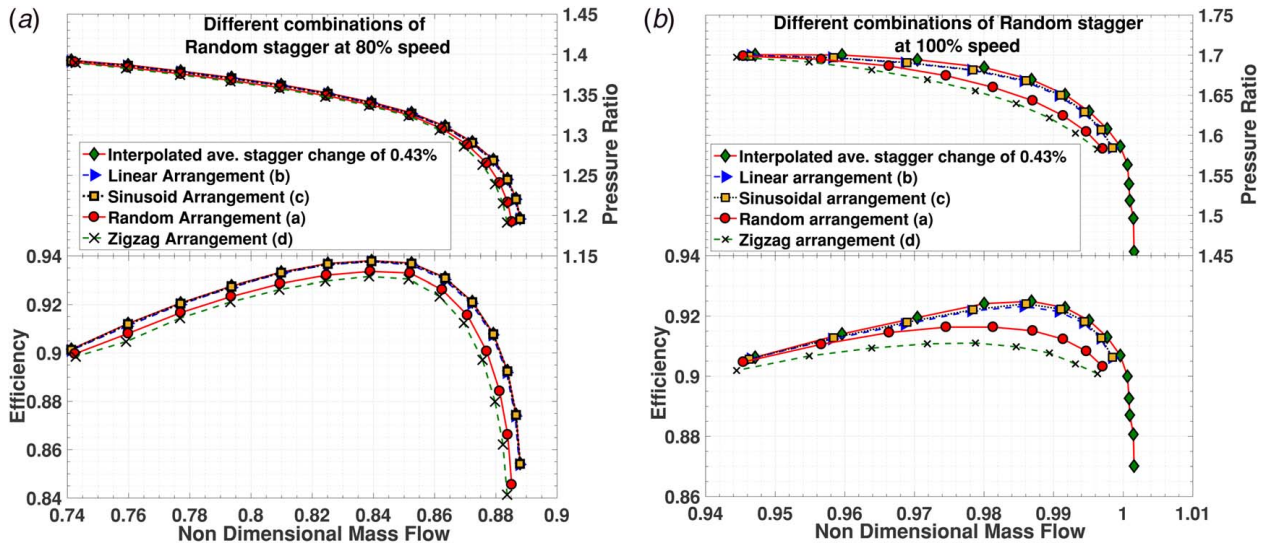

Fig. 10 Performance for different combinations of random stagger at (*a*) 80% fan speed and (*b*) 100% fan speed

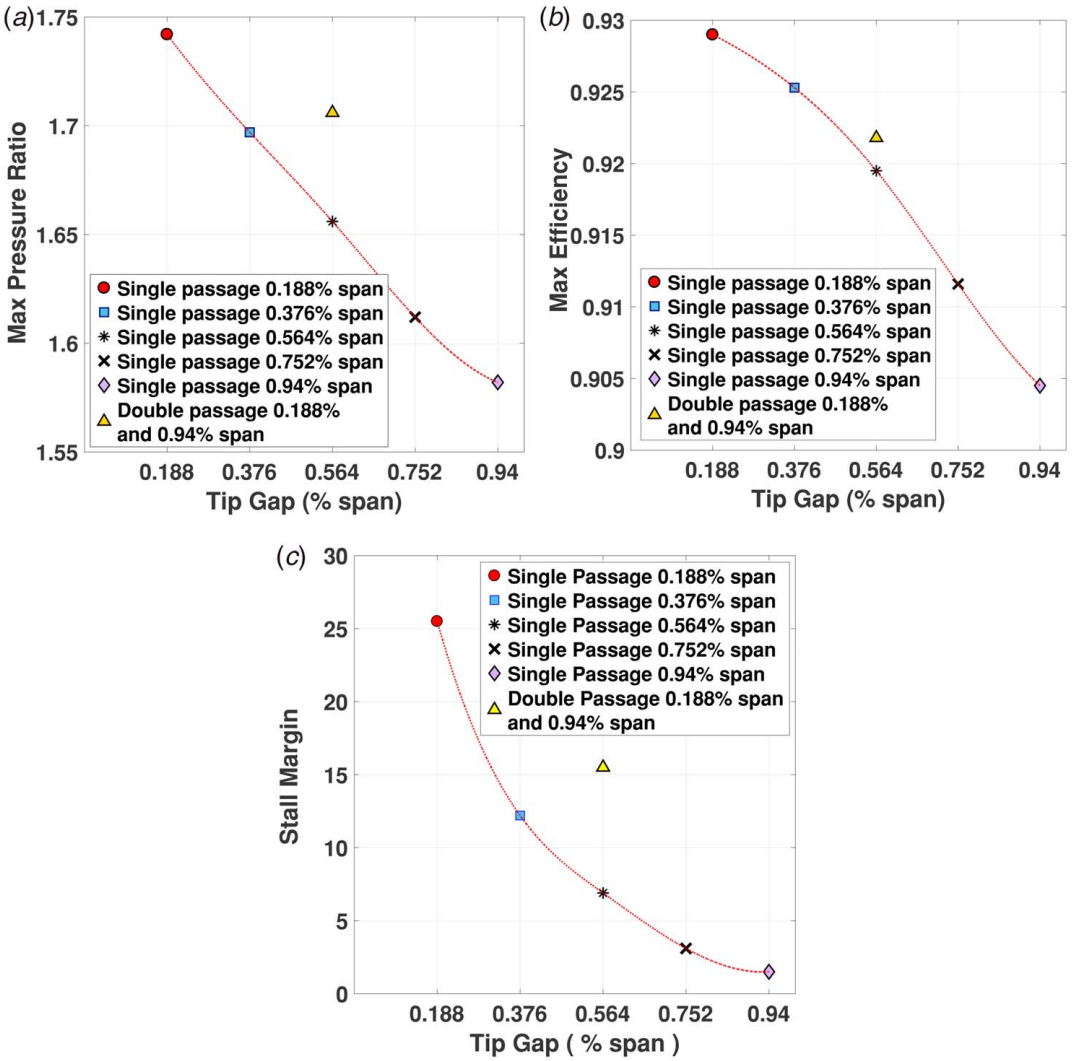

Fig. 11 (*a*) maximum pressure ratio with respect to tip gap, (*b*) maximum efficiency with respect to tip gap, and (*c*) SM with respect to tip gap

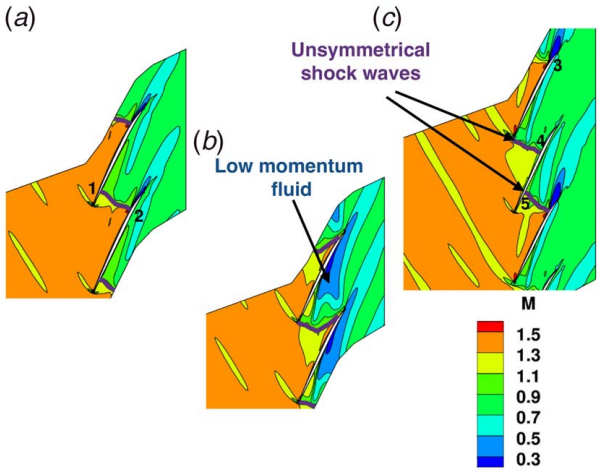

Fig. 12 Blade relative Mach number at 99% span at non-dimensionalized mass flowrate of 0.982 for different configurations: (*a*) single passage tip gap 0.188% span, (*b*) single passage tip gap 0.94% span, and (c) double passage tip gaps of 0.188% and 0.94% span

where **PR** is pressure ratio and $\dot{\mathbf{m}}$ is mass flowrate [23,24]. In addition to this, double passage rotor configurations with two different tip gaps for all the possible combinations from above tip gaps have been generated. As seen in the mesh convergence plot for various tips gaps shown in Fig. 3, an increase in tip gap size causes a decrease in pressure ratio, decrease in efficiency, and an increase in the stalling mass flowrate. These trends are shown in Figs. 11(*a*)–11(*c*) where the variation of maximum overall pressure ratio, maximum overall efficiency and SM is plotted against the tip gap size. Similar trends were obtained by Refs. [15,23,24]. Moreover, it can be observed from Fig. 11(*c*) that the **SM** is higher for double passage rotor with tip gaps of 0.188% span and 0.94% span compared to single passage with tip gap of 0.564%.

For brevity, the Mach number contours of only single passage tip gaps of 0.188% span, 0.94% span and double passage with tip gaps 0.188% span and 0.94% span together are shown in Figs. 12(*a*)–12(*c*). All the contours in Fig. 12 have been plotted at 99% span and a non-dimensional mass flowrate of 0.982 which are the points near peak efficiency. An increase in the tip gap causes the size and strength of tip leakage vortex to increase which in turn creates a large zone of low momentum fluid as seen in Fig. 12(*b*). It can also be seen from Fig. 12(*c*) that the low momentum fluid in double passage case with tips gaps 0.188% and 0.94% span is much smaller than single passage tip gap of 0.94% span. These pockets of low energy fluid produce a region of blockage which causes the main flow to be diverted around it. The altered main flow due to the blockage creates an adverse pressure gradient which leads to flow separation and hence the blade stall [24,25].

A schematic explanation of the mechanism of shock location for a single passage with tip gap of 0.188% span vis-a-vis a double passage with tip gaps of 0.188% and 0.94% together is shown in Fig. 13. Both of these cases are compared at same mass flowrate. A single passage case has a uniform mass flowrate from all its passage and thus has symmetric shocks in all the passages. In case of double passage, it can be seen that the higher tip leakage flow due to the larger tip gap blade causes the mass flowrate from one of the passages to drop thus pushing it towards stall. To compensate for this drop in mass flowrate, the other passage undergoes an increased mass flowrate thus causing it to become choked. Due to the location of shock waves in the double passage case, the larger tip gap blade becomes "unloaded" while the smaller tip gap blade becomes "more loaded" as seen in Figs. 14(*a*) and 14(*b*) wherein the blade loading of single passage tip gaps of 0.188% span and 0.94% span is compared with the individual blades of double passage tip gaps of 0.188% span and 0.94% span. These numbers marked (1–5) on this plot correspond to the numbers marked (1–5) on Mach number contours shown in Figs. 12(*a*)–12(*c*) at 99% span. Hence, in the presence of a blade with smaller tip gap, the blade with larger tip gap becomes less loaded than it would have been if all the blades had same tip gap size.

Another study was conducted to see the effects of arranging 11 blades of 0.188% span tip gap in one half of the annulus and 11 blades of 0.94% span tip gap in the other half of annulus (also called "half annulus arrangement") and was compared with double passage (zigzag pattern) tip gaps of 0.188% span and

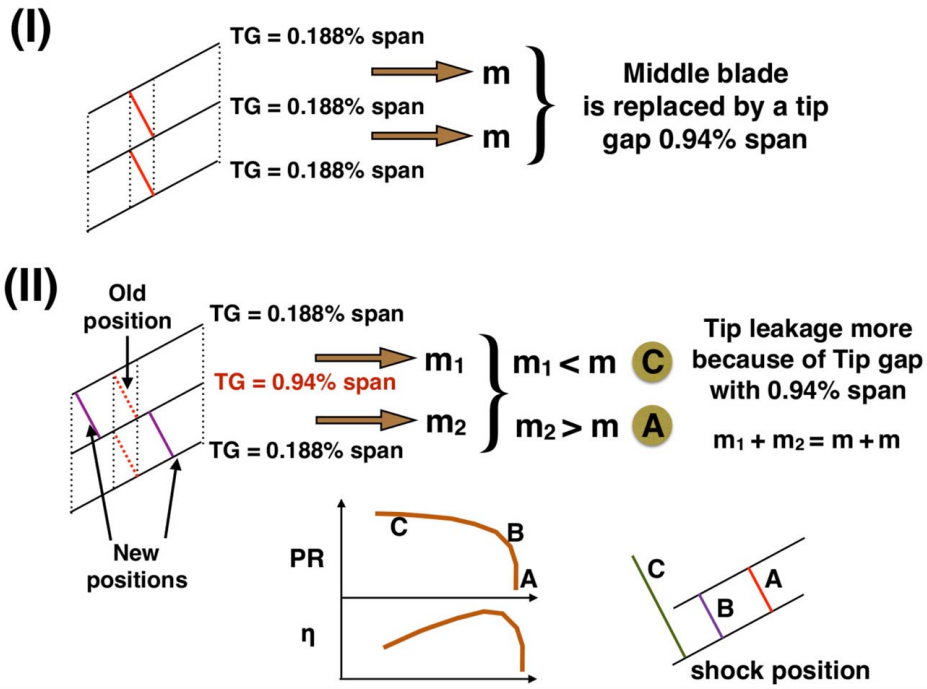

Fig. 13 Schematic showing location of shock in adjacent passage due to change in tip gap

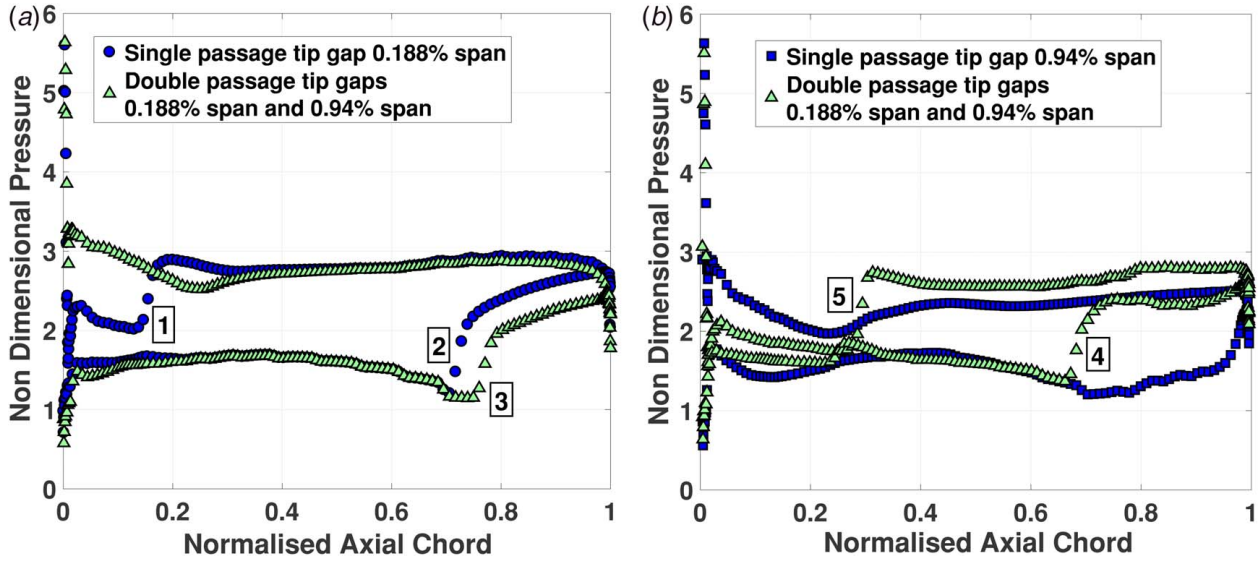

Fig. 14 (*a*) Comparison of 0.188% span tip gaps and (*b*) comparison of 0.94% span tip gaps. Comparison at 99% span of single passage blade with tip gaps 0.188% span and 0.94% with the respective individual blades of double passage blades with tip gaps 0.188% span and 0.94% span (near peak efficiency).

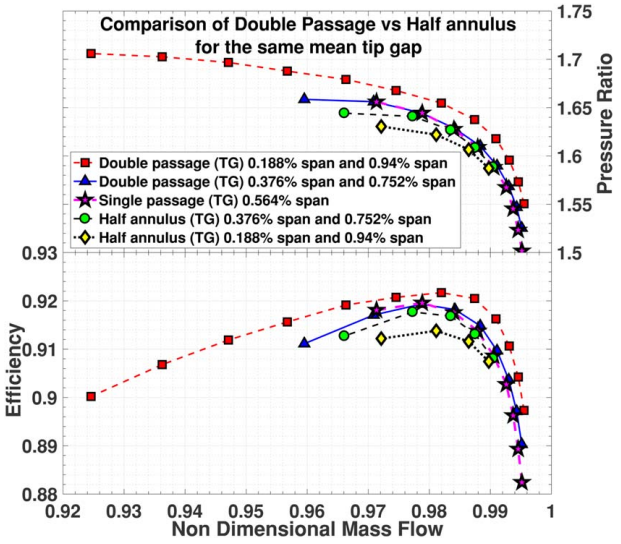

Fig. 15 Comparison of different double passage versus half annulus arrangement performances for the same mean tip gap

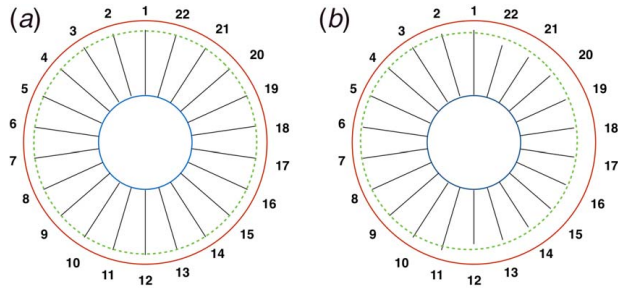

Fig. 16 A line diagram of compressor blades around the casing showing (*a*) uniform tip gap with concentric rotor and casing and (*b*) half annulus arrangement of different tip gaps producing an effect similar to eccentric rotor

0.94% span. It can be seen in Fig. 15 that the performance and the aerodynamic stability of the double passage with tip gaps 0.188% span and 0.94% span were much better than half annulus arrangement of the tip gaps 0.188% span and 0.94% span. Similar tests were performed for blades with tip gaps 0.376% span and 0.752% span. The performance of double passage with tip gaps 0.376% span and 0.752% span matches closely with the single passage tip gap of 0.564% span as does the half annulus arrangement of with tip gaps 0.376% span and 0.752% span. This implies that the type of arrangement plays no further role in eking out any extra performance when the manufacturing tolerance is very close to the mean value.

One interesting way to look at the uniform tip gap and half annulus arrangement case would be as shown in Figs. 16(*a*) and 16(*b*). It can be seen that the half annulus arrangement of non-uniform tip gaps introduces an effect similar to eccentrically mounted rotor which can be termed as induced eccentricity. In this regard, Graf et al. [1] conducted an experimental study on a subsonic axial compressor having a non-axisymmetric tip clearance. They observed that an eccentrically mounted rotor has a smaller stability margin compared to a rotor having uniform clearance of average same level. This is similar to the results shown in Fig. 15 wherein the half annulus arrangement with tip gaps 0.188% span and 0.94% span stalls earlier compared to single passage tip gap of 0.752% span. With a reduction of this induced eccentricity, the performance of half annulus arrangement with tip gaps 0.376% span and 0.752% span approaches the performance of single passage tip gap with 0.564% span. Graf et al. [1] have also tested the compressor for one lobed clearance asymmetry and two lobed clearance asymmetry which is akin to half arrangement and quadrant arrangement, respectively. Graf et al. [1] observed that two-lobe asymmetry performs better than one-lobe asymmetry. In the present paper, it is observed that the performance of the zigzag pattern (11 lobed) is much superior to that of half annulus arrangement (one lobe).

It can thus be hypothesized that when faced with random tip gaps in a whole annulus which are not close to mean value, the best arrangement would be to have a larger tip gap between two smaller ones also called as "zigzag arrangement" around the full annulus to obtain maximum efficiency, pressure ratio, and SM. The word "random" in the context of tip gaps is a slight misnomer as there are only five discrete tip gaps in this study. Instead, a uniformly distributed random integer between 1 and 5 was generated with "1" implying 0.188% span tip gap and "5" implying 0.94%

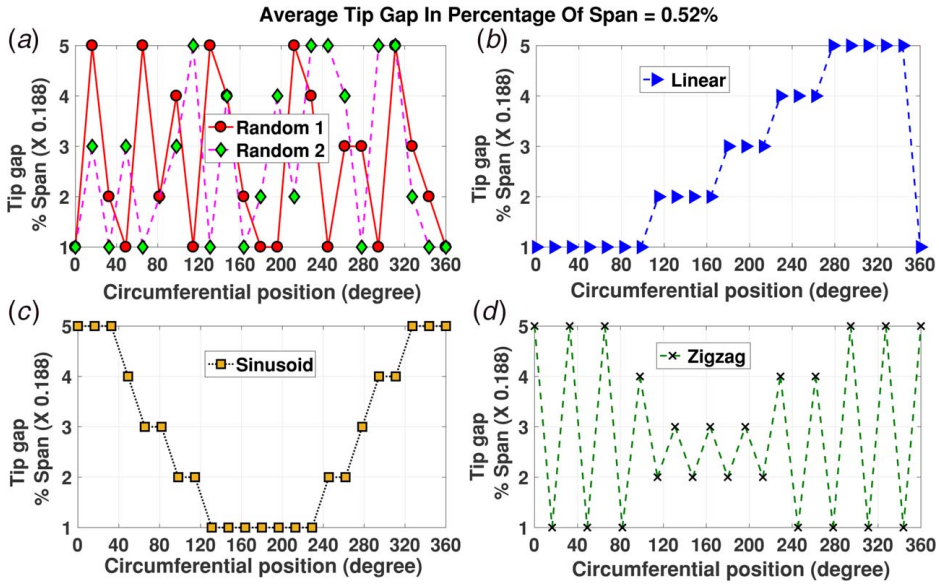

Fig. 17 Different combinations for same set of random tip gap blades with average tip gap of 0.52% span: (*a*) random arrangement, (*b*) linear arrangement, (c) sinusoid arrangement, and (*d*) zigzag arrangement

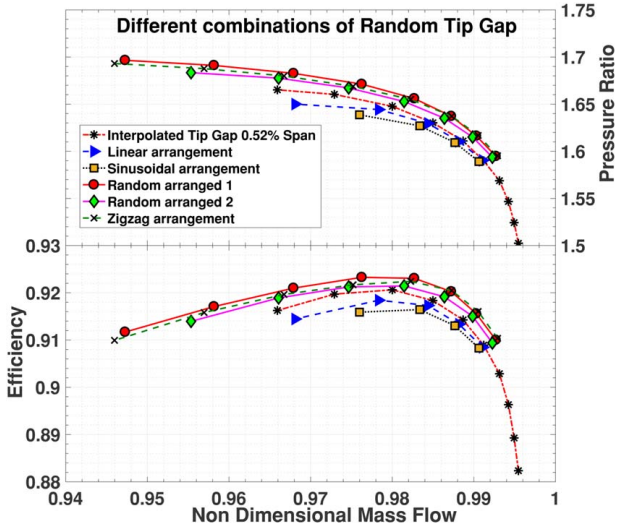

Fig. 18 Performance for different combinations of random tip gaps

span tip gap. Figure 17(*a*) shows the random arrangement of the different tip gaps while Figs. 17(*b*)–17(*d*) show the linear, sinusoid, and zigzag arrangement, respectively, for the same set of random blades. Figure 18 shows the corresponding performance of all the different arrangements described in Fig. 17. It can be seen that sinusoidal arrangement stalls earliest whereas the zigzag arrangement stalls the last on comparison with interpolated performance of single passage average tip gap of 0.52% span which implies that the performance of all the random combination lie in between these two extremities as seen from the performance of "Random arranged 1" and "Random arranged 2." It should be noted that for any arrangement, there are two combinations that are possible: (a) clockwise and (b) anticlockwise. There were no major difference in the performance curve exhibited by the two combinations. Future work would consider the effect of coupling between tip gap and stagger angle which is on the similar lines of the study by Montomoli et al. [26] and also develop a low fidelity model to predict the performance of compressors without resorting to full annulus simulation. Unsteady computations will also be performed to check the effect of optimized arrangement on the resulting aero-acoustics.

6 Conclusion

The study on the effect of manufacturing tolerance on the performance and stability boundaries of a compressor was carried out using stagger angle and tip gap variations as the parameters of interest. It was shown that in case of stagger angle, the change in passage area leads to the movement of the shock which affects the efficiency and pressure ratio. This change of passage area is minimum when the change in stagger between two successive blade is minimum. Hence, the most optimal arrangement when confronted with random stagger angle would be a sinusoidal arrangement wherein the circumferential variation is smooth throughout the annulus. A linear arrangement also gives a smooth circumferential variation bar, the variation between the first and the last blade. Performance wise, linear arrangement is equivalent to sinusoidal arrangement. In real turbomachinery application, the random stagger results would apply to both fan and compressors equally.

It was shown that in the presence of blades with smaller clearance next to ones with larger clearance, the loading on the blade with larger tip gap is reduced and thus stalling delayed. Hence, the most optimal arrangement when confronted with a random pattern of tip gaps is to arrange it in a zigzag arrangement wherein the larger tip gap blade is placed between two smaller tip gap blades. It was also seen that close manufacturing tolerance to the designed one would nullify the effect of different types of arrangements. In real turbomachinery application, the random tip gap results would be more significant in case of compressors. The results from simulation with random variation of tip gap can also be interpreted as the one with arrangement of blades having different SM (which can occur due to natural wear and tear over the course of engine operation). In such situations, the SM of the assembly can be improved with the suggested zigzag pattern during the overhauling and maintenance of engine. This study has neglected the weight imbalance issues that might arise while mounting of these blades. Considering it might result in an arrangement different from the one suggested in the paper. Also, the parameters like leading edge, camber, lean, and sweep have been neglected which can have pronounced effect on the optimal arrangement.

Acknowledgment

The first author would like to acknowledge the support provided by Reliance Industries Limited, India, for sponsoring this study.

Conflict of Interest

There are no conflicts of interest.

Data Availability Statement

The authors attest that all data for this study are included in the paper.

References

[1] Graf, M. B., Wong, T. S., Greizer, E. M., Marble, F. E., Tan, C. S., Shin, H. W., and Wisler, D. C., 1998, "Effects of Nonaxisymmetric Tip Clearance on Axial Compressor Performance and Stability," ASME J. Turbomach., **120**(4), pp. 648–661.

[2] Lange, A., Voigt, M., Vogeler, K., Schrapp, H., Johann, E., and Gummer, V., 2010, "Probabilistic CFD Simulation of a High-Pressure Compressor Stage Taking Manufacturing Variability into Account," Proceedings of ASME Turbo Expo 2010, Vol. 6: Structures and Dynamics, Parts A and B of Turbo Expo: Power for Land, Sea, and Air, pp. 617–628, Paper No. GT2010-22484.

[3] Montomoli, F., Carnevale, M., D'Ammaro, A., Massini, M., and Salvadori, S., 2015, *Uncertainty Quantification in Computational Fluid Dynamics and Aircraft Engines*, 2nd ed. (SpringerBriefs in Applied Sciences and Technology), Springer International Publishing, Heidelberg.

[4] Dodds, J., and Vahdati, M., 2015, "Rotating Stall Observations in a High Speed Compressor-Part 2: Numerical Study," ASME J. Turbomach., **137**(5), p. 051003.

[5] Vahdati, M., and Imregun, M., 1996, "A Non-Linear Aeroelasticity Analysis of a Fan Blade Using Unstructured Dynamic Meshes," Proc. IMechE Part C: J. Mech. Eng. Sci., **210**(6), pp. 549–564.

[6] Lee, K. B., Wilson, M. J., and Vahdati, M., 2018, "Validation of a Numerical Model for Predicting Stalled Flows in a Low Speed Fan—Part 1: Modification of Spalart–Allmaras Turbulence Model," ASME J. Turbomach., **140**(5), p. 051008.

[7] Wilson, M. J., Imregun, M., and Sayma, A. I., 2006, "The Effect of Stagger Variability in Gas Turbine Fan Assemblies," Proceedings of GT2006, Vol. 5: Marine; Microturbines and Small Turbomachinery; Oil and Gas Applications; Structures and Dynamics, Parts A and B of Turbo Expo: Power for Land, Sea, and Air, pp. 1059–1069, Paper No. GT2006-90434.

[8] Vahdati, M., Sayma, A. I., Freeman, C., and Imregun, M., 2004, "On the Use of Atmospheric Boundary Conditions for Axial-Flow Compressor Stall Simulations," ASME J. Turbomach., **127**(2), pp. 349–351.

[9] Sayma, A. I., Vahdati, M., Sbardella, L., and Imregun, M., 2000, "Modeling of Three-Dimensional Viscous Compressible Turbomachinery Flows Using Unstructured Hybrid Grids," AIAA J., **38**(6), pp. 945–954.

[10] Arima, T., Sonoda, T., Shirotori, M., Tamura, A., and Kikuchi, K., 1999, "A Numerical Investigation of Transonic Axial Compressor Using a Low-Reynolds-Number $\kappa-\epsilon$ Turbulence Model," ASME J. Turbomach., **121**(1), pp. 44–58.

[11] Choi, M., Baek, J. H., Park, J. Y., Oh, S. H., and Ko, H. Y., 2010, "Effects of Low Reynolds Number on Loss Characteristics in Transonic Axial Compressor," Trans. Jpn. Soc. Aero Space Sci., **53**(181), pp. 162–170.

[12] Jennions, I. K., and Turner, M. G., 1993, "Three-Dimensional Navier-Stokes Computations of Transonic Fan Flow Using an Explicit Flow Solver and an Implicit κ–ϵ Solver," ASME J. Turbomach., **115**(2), pp. 261–272.

[13] Strazisar, A. J., Wood, J. R., Hathaway, M. D., and Suder, K. L., 1989, "Laser Anemometer Measurements in a Transonic Axial-Flow Fan Rotor," Technical Publication NASA-TP-2879, Lewis Research Center, NASA, Cleveland, OH, November.

[14] Roberts, W. B., Thorp, S. A., Prahst, P. S., and Strazisar, A. J., 2013, "The Effect of Ultrapolish on a Transonic Axial Rotor," ASME J. Turbomach., **135**(1), p. 011001.

[15] Adamczyk, J. J., Celestina, M. L., and Greizer, E. M., 1993, "The Role of Tip Clearance in High-Speed Fan Stall," ASME J. Turbomach., **115**(1), pp. 28–38.

[16] Crawley, E. F., and Mokadam, D. R., 1984, "Stagger Angle Dependence of Inertial and Elastic Coupling in Bladed Disks," ASME J. Vib. Acoust. Stress Reliab., **106**(2), pp. 181–188.

[17] Stapelfeldt, S. C., 2014, "Advanced Methods for Multi-row Forced Response and Flutter Computation," PhD thesis, Imperial College London, London, January.

[18] Sladojevic, I., Sayma, A. I., and Imregun, M., 2007, "Influence of Stagger Angle Variation on Aerodynamic Damping and Frequency Shifts," Proceedings of GT2007, Vol. 5: Turbo Expo 2007 of Turbo Expo: Power for Land, Sea, and Air, pp. 683–700, Paper No. GT2007-28166.

[19] Zheng, S., Fan, L., Teng, J., and Qiang, X., 2017, "The Impact of Uncertain Stagger Angle Variation on High-Pressure Compressor Rotor Performance," Proceedings of Shanghai 2017 Global Power and Propulsion Forum, pp. 1–7, Paper No. GPPS-2017-0045.

[20] Bazovsky, I., 2004, *Reliability Theory and Practice*, Dover Publication Inc, Mineola, NY.

[21] Park, S. Y., and Bera, A. K., 2009, "Maximum Entropy Autoregressive Conditional Heteroskedasticity Model," J. Econ., **150**(2), pp. 219–230.

[22] Lu, Y., Green, J., Vahdati, M., and Stapelfeldt, S. C., 2018, "Effect of Geometry Variability on Fan Performance and Aeromechanical Characteristics," Proceedings of 15th International Symposium on Unsteady Aerodynamics, Aeroacoustics and Aeroelasticity of Turbomachines, pp. 1–9, Paper No. ISUAAAT15-095.

[23] Moore, R. D., 1982, "Rotor Tip Clearance Effects on Overall and Blade-Element Performance of Axial-Flow Transonic Fan Stage," Technical Publication NASA-TP-2049, Lewis Research Center, NASA, Cleveland, OH, September.

[24] Beheshti, B. H., Farhanieh, B., Teixeira, J. A., Ivey, P. C., and Ghorbanian, K., 2004, "Parametric Study of Tip Clearance-Casing Treatment on Performance and Stability of a Transonic Axial Compressor," ASME J. Turbomach., **126**(4), pp. 527–535.

[25] Thompson, D. W., King, P. I., and Rabe, D. C., 1998, "Experimental Investigation of Stepped Tip Gap Effects on the Performance of a Transonic Axial-Flow Compressor Rotor," ASME J. Turbomach., **120**(3), pp. 477–486.

[26] Montomoli, F., Massini, M., and Salvadori, S., 2011, "Geometrical Uncertainty in Turbomachinery: Tip Gap and Fillet Radius," Comput. Fluids, **46**(1), pp. 362–368.